In-situ Fiber Strength Distribution In Nextel™ 610 Reinforced Aluminum Composites

Joe Butler

Thesis submitted to the Faculty of the
Virginia Polytechnic Institute and State University
in partial fulfillment of the requirements for the degree of

MASTER OF SCIENCE

in

Materials Science and Engineering

Approved by:
Dr. Steve Kampe, Chairman
Dr. Jean Kampe
Dr. Norman Dowling

April 26, 2006
Virginia Tech
Blacksburg, VA

Keywords: Metal Matrix Composites, Nextel 610™, MetPreg™ Composite Tape, Single Fiber Testing, Strength Distribution of Fibers, Fracture Toughness, Weibull Modulus

In-situ Fiber Strength Distribution
In
Nextel™ 610 Reinforced Aluminum Composites

Joe Butler

Abstract

MetPreg, a composite developed by Touchstone Research Laboratories (Tridelphia, WV), is an aluminum metal matrix composite reinforced by continuous Nextel™ 610 alumina fibers. The question is, after processing, are the Nextel™ fibers affected in any way that their strengthening contribution to the composite is reduced? From experimentation and statistical analysis, a strength distribution of pre-processed Nextel™ 610 fibers is formed and an empirical correlation is developed relating strength to the observed flaw size on the failed single fibers. This correlation is then independently applied to flaw size information gathered from fibers on the fracture surface of MetPreg samples to develop a separate strength distribution of post-processed Nextel™ 610 fibers. The pre- and post-processed distributions are compared to one another to determine the effect, if any, that composite processing has on the strength of Nextel™ 610 fibers.

Acknowledgements

I would like to thank my advisor Dr. Stephen Kampe for all of his guidance throughout this research work. I also want to thank my committee members Dr. Norman Dowling and Dr. Jean Kampe for answering all the questions I had and their advice and comments regarding this project.

A special thanks to Dr. Jeff Schultz for his suggestions in modifying the fiber testing method and for showing me how to use the equipment involved with testing, and to Steve McCartney for all of his help in teaching me how to use the SEM.

Also, thanks Touchstone Research Laboratory for supplying the tow of Nextel™ 610 fibers and MetPreg™ composite tape tested in this project.

I also want to give thanks to undergraduates involved with this research. To Dan Durrbeck and Sara Hix, whose senior design project lead into the basis for my experimental method and testing technique. To Jenny Mueller, for without whose time and steady hand in sample preparation, I doubt I would have gathered as much data as I did.

To my fellow graduate students in the Kamposites group, thanks for all the helpful comments and camaraderie, grad school here at VT has been fun.

Last, and definitely not least, to my family for supporting my decision to go to graduate school and believing in me, and my friends for having faith that I could pull this off.

Table of Contents

List of Figures

List of Tables

Chapter 1: Background

1.1 Introduction

MetPreg™ composites produced by Touchstone Research Laboratory Ltd (Tridelphia, WV) are one example of many types of metal matrix composites (MMCs) being developed for structural applications. MMCs are being explored for a multitude of applications, and like most composites offer the benefit of being capable of being engineered and tailored to fit these applications. In particular, parts composed of MetPreg™ composite tapes are being explored for possible application as storage tanks and pressure vessels, lightweight structures for various vehicle frames, and potentially even as material to selectively reinforce existing metal structures. The potential of fiber reinforced composites is as varied as the reinforcements themselves. Fibers can be produced with many different characteristics that can be beneficial to the intended matrix and application.

1.2 Fiber Characteristics

There are a wide array of fibers that have been developed for the purpose of composite reinforcement. A fiber's performance for composite reinforcement differs in many aspects by way of its size, shape, and composition. Aspects of fiber processing also play a role in the fibers' purity and defects that can affect its quality and usefulness. Each type of fiber is designed to best utilize the component material's properties and contour it to the particular application intended for a composite material.

A fiber's size has many effects upon its characteristics and properties. As the diameter of a fiber decreases, its strength tends to increase. The reduction in size relates to a fiber's probability of survival, since smaller flaws correlate to a higher strength at failure whereas fibers with larger flaws fail at lower strengths, thus having a lower probability of survival. Generally this is also attributed to the fact that smaller diameter fibers have reduced or even eliminated surface defects entirely in the production process [1]. Also, smaller diameter fibers result in increased loading efficiency. For a given volume of reinforcement in the matrix, with smaller diameters the edge to edge spacing between fiber reinforcement is reduced. A fiber's length plays a role as much as

diameter. A fiber's critical length is a characteristic associated with a fiber's ability to become fully loaded. Since stress develops from each end of a fiber towards the midpoint, small diameter fibers do not require large lengths to achieve the critical length, which leads to how influential a fiber's aspect ratio can be [2].

The length of fiber reinforcements also plays a role on the processing of a composite. With short or discontinuous fibers, it becomes a matter of simply adding a desired amount of reinforcement to a batch of matrix material for manufacturing, and then forming the composite product. This processing advantage for discontinuous fibers, however, results in the disadvantage that reinforcement orientation is random. In the case of continuous reinforcement, specific equipment and design processes involving mandrels and pulling devices take a bundle or tow of fibers and usually pull a continuous reinforcement through a molten bath of matrix material to form composites. For continuous reinforcement, orientation and distribution within a matrix is more defined, which can result in better and more consistent mechanical properties [1].

Fiber reinforcement's shape also has influences on its properties. Most fibers are produced with circular cross sections, but through different processing techniques, such as using a different shape die in melt spun methods, fibers of different cross sections can be achieved including hexagonal, rectangular, polygonal, irregular shapes, and even hollow fibers [1]. With the development of different shaped fibers, their use as reinforcement and what benefits one shape has over another as reinforcement in possible composite applications are being explored. Figure 1 displays and compares various different cross sectional shapes of fiber reinforcements.

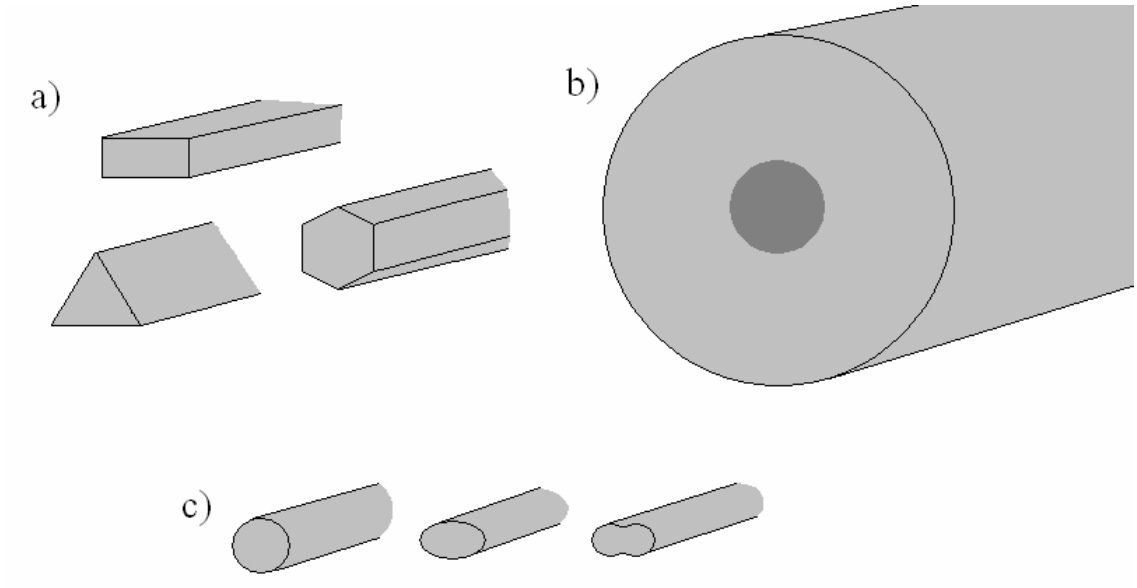

Figure 1 A comparison of various cross sectional shapes of fiber reinforcements. a) Different polygonal shapes seen with single crystal fibers; b) multiphase fibers, such as Boron and certain SiC fibers, formed by vapor deposition onto a substrate core. Fibers can range from 100 - 200 μm in diameter for use as reinforcement; c) Circular and ellipsoid shapes are common with drawn or spun fibers. These have been seen on the order of 10-20 μm [1]

As observed, a wide array of fibers are available as reinforcement for composite materials. In the case of aluminum MMCs, a variety of continuous fiber reinforcements have been explored. Continuous fibers are of more interest because of their greater potential for strengthening, and then take advantage of new innovations in manufacturing processes of aluminum MMCs. One such example of these composites is MetPreg™ tapes produced by Touchstone Research Laboratory (TRL), made with continuous alumina fibers. There are various continuous fiber reinforcements that have been used for aluminum MMCs, which have included boron, silicion carbide, aluminosilicates, as well as alumina fibers. These fibers are produced by a variety of methods based upon their composition and, in turn, these materials have different properties. It is of interest to understand the differences between these types of reinforcements and to better understand why TRL chose alumina fibers as the reinforcement for their MetPreg™ tapes. Table 1 shows some examples of different fibers, comparing their properties and common diameters. The sections that follow provide more detail regarding their production and characteristics.

Table 1 Comparison of typical sizes and properties of various commercially available continuous fiber reinforcement used in aluminum metal matrix composites [1, 3-5].

	Boron	Silicon Carbide	Aluminosilicates	Alumina
Diameter size (μm)	95 - 200	10 - 20	2.5 - 5.5	10 - 12
Melting Point (^{o}C)	1260	2690	1760	2040
Tensile Strength (GPa)	3.4 – 3.9	3.9	1.6 – 2.5	2.1 - 3.1

1.3 Boron Fibers

Composite fiber reinforcements comprised of boron have been attractive for use with aluminum MMCs because of their excellent mechanical properties coupled with their low density. The production cost associated with boron fibers is very high. As a result, these fibers have been seen used mainly as composite reinforcements where lightweight, high strength, and high modulus values are necessary. However, these fibers are limited because of their large diameters, how their strength decreases at increased temperatures, and the poor stability they exhibit in metal matrices [3]. Boron fibers are generally produced through a vapor-deposition process where boron is coated onto a core of either tungsten or carbon fiber [5]. Continuous pure boron fibers were attempted in early manufacturing but had very little application because they were found to be too brittle.

For both types of cores, the vapor deposition processes used to form the boron fibers are similar. The process begins with the core fiber being drawn off a spool and carried through a pretreatment chamber through a mercury seal. In the case of tungsten-core fibers, they are normally heated to around 1200^{o}C in an atmosphere of hydrogen to remove any surface oxides and impurities. The carbon-core fibers undergo a thin coating of pyrolytic graphite by exposure to a mixture of methane, argon, and hydrogen at temperatures up to 2500^{o}C as its pretreatment step. [3] Once pretreated, the core fibers are then transported to the depositing chamber. At approximately 1150^{o}C, the fibers are then resistively heated with an electrical current in an atmosphere containing a mixture of hydrogen and BCl_3. The following equation describes the characteristic reaction that takes place in boron deposition:

$$2BCl_3(g) + 3H_2(g) \rightarrow 2B(s) + 6HCl(g) \quad [3]$$

After the boron deposition reaction, the fibers are then wound onto another spool and sent to successive reaction chambers to reach diameter range of 100 to 200 μm [3]. The microstructure and chemical compositions of the boron deposited fibers are quite different between the two substrates, with there being no significant reaction with the carbon core and the formation of the W_2B_5 and WB_4 borides from the tungsten core [5]. In the case of the carbon core fibers, the microstructure of the boron fibers is dense with boron nucleating out from the carbon core and usually results in a smooth fiber surface. Boron fibers developed from tungsten cores tend to form a nodular structure with the different boride formation which causes the fibers to have a relatively rough surface.

A series of post treatments are usually performed to improve different characteristics that are due to the deposition and reaction process [5]. Heat treatments are performed to remove any residual stresses, from the core interface out toward the fiber surface, that may have developed in processing due to the volume changes that occur during formation. Chemical treatments are usually performed to remove any surface defects that may have developed. The outer surface of these fibers is comprised of boric oxide, providing some oxidation resistance but this resistance is lost at high temperatures.

These fibers are particularly used for lightweight composites and have seen applications in sports equipment to aircraft [3]. However, their large diameter sizes, which can range from 95 to 200 μm when manufactured for the purposes of composite reinforcement, limit the potential of these fibers. Such large fibers have the drawback of being lower in strength relative to fibers of smaller diameters. Another issue is the reactive nature of boron with most metals, which again prohibits the use of the fibers unless special coatings are applied to the surface. These surface coatings are at times necessary, to not only aid in the fiber's oxidation resistance but also to improve their compatibility with metal matrices for composite manufacture.

1.4 Silicon Carbide Fibers

Silicon Carbide (SiC) fibers are in large part designed and developed for use as reinforcement for MMCs. These fibers are usually characterized by having high strength, high stiffness, and low density [5]. These fibers also exhibit higher temperature resistance than boron fibers due to their excellent oxidation resistance at elevated

temperatures. Even at exposure to high temperatures, these fibers retain the majority of their tensile strength and modulus properties. SiC fibers have been observed as having superior compressive strength, electrical resistance, and oxidation resistance at high temperatures than compared to many other fibers, making them more advantageous in given applications [3].

There are two different processes used in producing SiC fibers commercially. One method involves taking a tungsten or carbon filament and coating it with SiC by vapor deposition. This method is very similar to the deposition method for the development of boron fibers, with the substrate usually being a spun carbon monofilament on the order of 33 μm in size [5]. The fibers produced through vapor deposition tend to have diameters from 100 to 150 μm. The second method for SiC production involves a melt spun process. An organic polymer containing silicon atoms is melt spun and used as a precursor fiber, which is then heated at an elevated temperature to produce fibers with diameters between 10 to 20 μm [3].

As mentioned before, SiC fibers have highly desirable mechanical properties as composite reinforcement and can be used to elevated temperatures. These fibers have the advantage of being more oxidation resistant than boron and even regular carbon fibers. SiC fibers can be used in applications as high as 1800^{o}C, but the tensile strength and modulus properties deteriorate at temperatures above 1200^{o}C [3, 5]. This temperature is not necessarily an issue for aluminum MMCs. For the purposes of reinforcement in aluminum MMCs, SiC fibers exhibit excellent qualities and properties. The ultimate drawback however, is not SiC fibers' properties, but the cost associated with producing these fibers.

1.5 Aluminosilicate Fibers

Aluminosilicate fibers are metal oxide fibers comprised of both Al_2O_3 and SiO_2. This group of fibers can be divided even further into fibers that can be melt-spun and those that cannot. Aluminosilicate fibers containing a percentage of 40 to 65 wt% Al_2O_3 can be melt spun into continuous fibers due to the higher concentration of SiO_2 in the mixture which allows for a lower melting point and higher viscosity of the mixture [3].

The melt spun method of producing aluminosilicate fibers is straightforward. The raw materials used are from kaolin or similar clays containing Al_2O_3 and SiO_2. The clay material is melted and then discharged through an opening in the bottom of the melt chamber. The molten material is fed downward to a rapidly rotating disk that is oriented vertically. As the material falls onto the rapidly rotating disk, the fibers are spun via the centrifugal force [3]. This method produces longer and finer fibers than other forming methods for aluminosilicate fibers, with diameters ranging from 1-10 μm. The limits of aluminosilicate fibers are based largely upon the composition, with higher Al_2O_3 content fibers having higher temperature capabilities. Fibers containing approximately 50% Al_2O_3 are suitable as insulation for temperatures up to 1250^{o}C and fibers with as high as 65% Al_2O_3 can be used in applications up to 1400^{o}C [3].

The quality of fiber production is an issue, for there needs to be a certain level of homogeneity with continuous fibers used as reinforcement. Though there is potential for these fibers as reinforcement, the majority of continuous aluminosilicate fibers are used in the production of yarns designed to be woven into insulating fabrics where the need for consistent fibers is not as stringent. The composition of aluminosilicate fibers results in mechanical properties that are not effective of as composite reinforcement. This can mostly be attributed to the creep characteristics of aluminosilicates, which limits their use in composites for high stress applications at elevated temperatures.

1.6 Alumina Fibers

A need for higher modulus of elasticity, melting point, and exceptional resistance to corrosive conditions resulted in manufacturing fibers of pure or near pure Al_2O_3 [6]. These relatively pure alumina fibers contain very little if any SiO_2 and other components within the fiber's composition. As a result, alumina fibers cannot be melt-spun due to the high melting point and low viscosity and thus alternate forms of processing are used. One method involves taking aluminum salts and dispersing them in a precursor fiber, heating the fibers to burn off the organic material of the precursor fiber, and lastly sintering the fiber to produce the final Al_2O_3 fiber [3]. The processes of slurry and sol-gel processing are two other methods developed for the commercial production of alumina fibers.

The slurry processing technique involves great care in slurry creation, fiber extrusion, and sintering. An aqueous suspension of Al_2O_3 particles containing dissolved organic polymers is prepared [3]. The organic polymer is used in the slurry suspension to aid in increasing the viscosity and stabilizing the suspended particles. Additional additives can be added to aid in minimizing grain growth and increase densification during sintering. Once the slurry is prepared it is extruded in air, allowed to dry, and then sintered at low temperatures to allow for some shrinkage without distorting the fibers. In the last stages of production, the fibers are flame fired to reduce and eliminate any porosity and produce alumina fibers that are comprised almost entirely of the α-Al_2O_3 phase, which is desired for its high modulus and high temperature resistance [3].

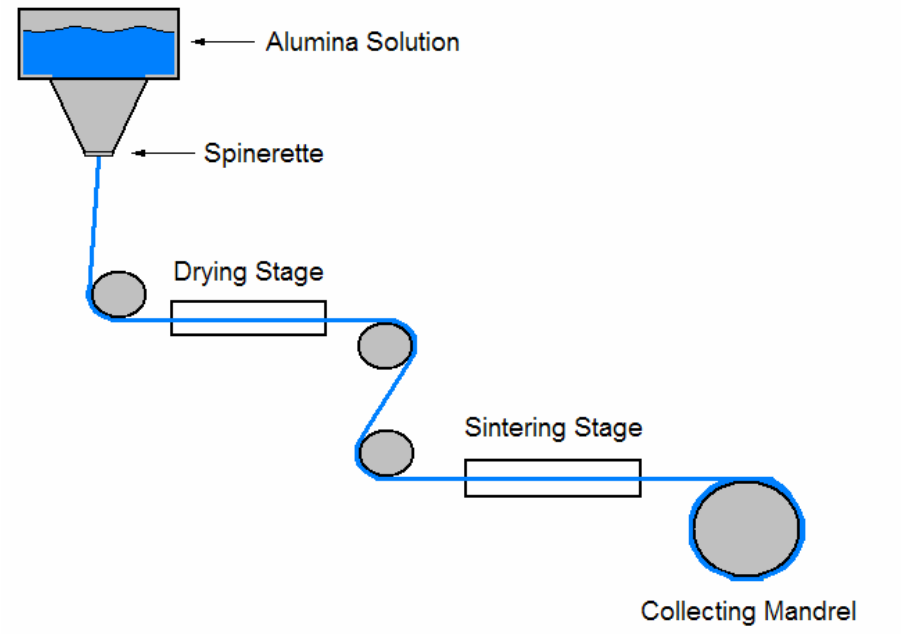

Figure 2 Generic schematic displaying the stages involved with the sol-gel processing for producing alumina fibers.

The sol-gel processing technique for alumina fibers involves taking solutions of high concentrations of aluminum compounds and spinning fibers from this solution. Water or an organic solvent may be used in the spinning solution. Spinning solutions comprised of aqueous solutions contain basic aluminum chlorides with additional water-soluble polymers to control the rheology of the solution. Additional additives are used to also control grain growth and phase stabilization [3]. Once prepared, the solution is then

extruded into air or onto a rotating disk. The fibers are then subjected to increasing temperatures to burn off organic matter and remove HCl from the aluminum chlorides. After the removal of these constituents, an amorphous Al_2O_3 phase forms. As the temperature continues to increase, the alumina becomes crystalline, undergoing different phase changes until it reaches the desired stable α phase. The first Al_2O_3 phase to form is η and, as the temperature decreases, changes and continues through to γ, δ, θ, and finally the composition becomes α phase.

The α phase of Al_2O_3 is desired for fibers used in composites with high temperature applications due to its higher temperature resistance and modulus value. However, with the increasing temperature, the not only are there phase changes within the material, but the grain size changes as well. With increased temperatures the grain size increases, and this increased size decreases the tensile strength of the material. To counter this crystal growth, small amounts of additives including acidic oxides of silicon, phosphorous, boron, and zinc are used [3]. By controlling these additives and temperatures, the desired properties can be attained for alumina fibers through sol-gel processing. The diameter size of the fibers affects the properties of the fiber, with smaller diameters resulting in increased tensile strength of the fibers. It is through sol-gel processing that 3M Corporation produces the Nextel™ family of fibers.

1.7 Nextel Family of Alumina Fibers

Nextel™ 610 is one amongst a group of aluminum oxide fibers specifically designed for use as reinforcement in ceramic and metal matrix composites. 3M™ Manufacturing has developed three different fibers in the Nextel™ series tailored for the express purpose of composite reinforcement, Nextel™ 610, 650, and 720. All three continuous fibers are designed as composite reinforcements, but their compositional differences result in differing properties. Nextel™ 610 was designed to have higher strength characteristics but is susceptible to creep at elevated temperatures. Nextel™ 720 was then designed to have better creep resistance for elevated temperature applications, but was reduced in strength. The Nextel™ 650 series was designed to be a 'middle of the road' fiber that had greater strength than 720 but still retained better creep resistance properties than 610. The Nextel™ series of fibers being mostly comprised of Al_2O_3 are

produced via sol-gel processing, which in turn makes them less expensive to produce than some other fibers, such as SiC.

Table 2 Comparison of properties of Nextel™ fibers designed for use as composite reinforcements [4, 7]

Nextel™ Properties	610	650	720
Composition	>99 w% Al_2O_3	89 w% Al_2O_3 10 w% ZrO_2 1 w% Y_2O_3	85 w% Al_2O_3 15w% SiO_2
Crystal Phase	α Al_2O_3	α Al_2O_3 + cubic ZrO_2	α Al_2O_3 + mullite
Diameter (μm)	10-12	10-12	10-12
Single Fiber Strength (GPa)	3.1	2.5	2.1

The high strength of Nextel™ 610 fibers is one of its primary characteristics that make it appealing as reinforcement for composites. In the case of aluminum metal matrix composites, the fiber reinforcement is used to strengthen and stiffen the composite relative to the matrix [8]. The high strength of Nextel™ 610 fibers are attributed in part to the fine grain structure of the material that is achieved through careful control of the processing technique. Nextel™ 610 fibers are comprised almost entirely of a pure α Al_2O_3. These fibers are produced through a sol/gel processing technique. However, it is not a simple matter to process α Al_2O_3 into fiber form based upon its low volumetric nucleation density, which is the reason that α Al_2O_3 tend to have large grain sizes. Large grain sizes, along with the high levels of porosity that can result during crystallization, are counter to attaining the desired high strength for the reinforcement. The minimization of defects or flaws during formation is also of concern during fiber processing. Ideally, a homogeneous fine grained microstructure coupled with high density is desired. Sol/gel processing is the technique found most effective for producing such desired characteristics. Through proper use of nucleation agents and careful control during processing, Nextel™ 610 fibers are produced with a uniform microstructure comprised of grains 0.1 μm in size and little porosity [8].

1.8 MetPreg™ Composite

MMC materials display great potential because in comparison to polymer matrix composites (PMCs), MMCs are capable of exhibiting higher values of fracture toughness, greater transverse stiffness, and higher strength properties [1]. Also, MMCs tend to have better environmental resistances, notably in high temperature applications. They tend to show no moisture absorption or outgassing, and little material degradation in comparison to PMCs [9]. Some of the advantages of using a metal matrix composite over a product comprised of just metals are more desirable mechanical and thermal properties as well as the ability to better tailor a material for a specific application. Many metals and metallic alloys could be used as matrices for composite materials, however the choices are usually based on aspects of the intended application, such as weight restrictions and temperature. Metals that are commonly used as matrices include aluminum, titanium, magnesium, and their alloys [1].

MetPreg™ is an aluminum metal matrix composite developed by Touchstone Research Laboratory Ltd. The choice of aluminum and aluminum alloys as matrices over other metals is based on its light weight. When being compared to a polymer prepreg composite, an aluminum matrix still offers a lightweight material while bringing in the advantages of a metal. It is not as sensitive to conditions like moisture and temperature as some polymers matrices. MetPreg™ as a material combines the lightweight characteristics of aluminum metal with the desirable properties of high strength, high modulus, and greater stiffness of Nextel™ 610 aluminum oxide fibers, while making use of an already existing manufacturing process designed for polymer prepregs.

TRL has developed a manufacturing process for producing MetPreg™ tape. It involves passing fiber tows through a bath of molten aluminum where the metal infiltrates between the fibers in the bundle. This infiltrated tow then passes through a shaping die to reach the desired shape and is then cooled to produce the final MetPreg™ composite [9]. Figure 3 schematically displays this process.

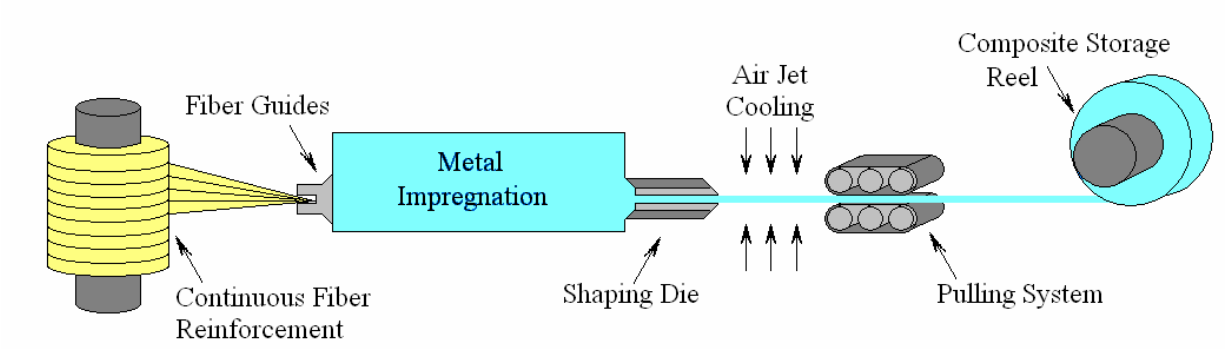

Figure 3 Schematic displaying the pultration processing technique for producing MetPreg™ tape [9].

The processing technique is similar to those used in the manufacture of PMC prepregs. This pultrusion technique has a flexible setup, allowing for different shape adaptations for composite manufacture. Some standard pultrusion profiles include rectangular and round tubes, channels, and angles in addition to tapes [9]. The tapes are nominally produced with a 50 volume percent fiber content, although tapes containing up to 60 volume percent have been produced with dimensions ranging from 0.15 to 0.50 mm in thickness and 10 to 40 mm in width [9]. The flat tapes are wound onto storage reels until used in fabrication stages for various parts, whereas the other shapes are cut to the desired length and stacked.

Actual part production using MetPreg™ tapes involves two main stages, the part build-up and the part consolidation. The build-stage involves arraying MetPreg™ tapes either by hand or an automated process to form a specific multilayered, multidirectional part. Tapes are aligned in a fixture, using either brazed coated tapes or thin sheets of filler metal between the layers. After a formation, the part is consolidated by one of the following processes: vacuum bagging, hot pressing, hot isostatic pressing (HIP), or adhesive bonding, brazing, soldering and welding [9].

TRL implements and adapts some of the common consolidation techniques for the manufacture of parts comprised of MetPreg™ tapes. One such device that has been developed makes use of traditional PMC tape placement processing with the modification of a laser to continuously consolidate the MetPreg™ pieces [9]. A basic schematic of the process is shown in Figure 4. This process makes a part that is positioned on a rotating mandrel. As the mandrel rotates, a laser creates a localized heating area where the

coating layer is heated to its melting point and compacted to the previous layer, forming a bonded cylinder composed of the MetPreg™ tapes.

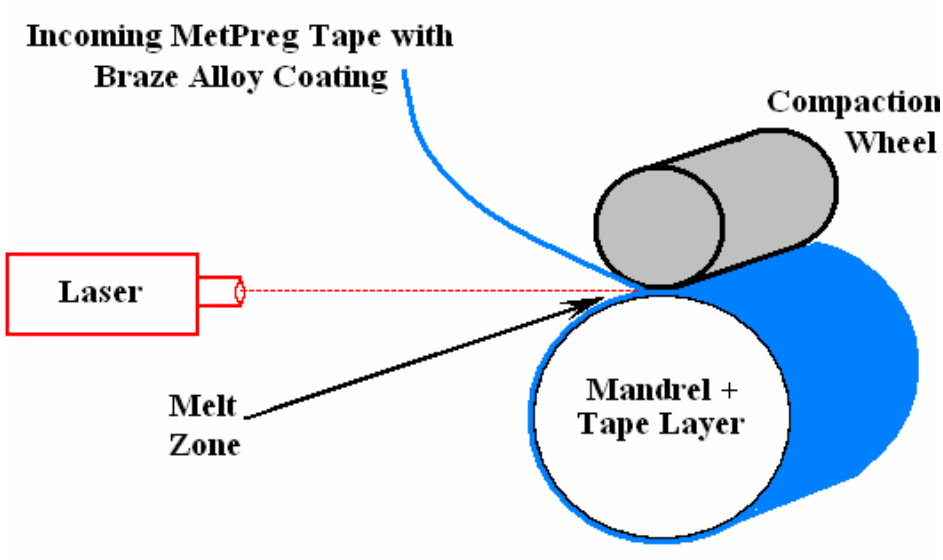

Figure 4 Sketch of the continuous tape placement process by Touchstone Research Laboratory Ltd [9]

1.9 Fiber Degradation

As previously stated, the whole purpose of adding continuous fiber reinforcement is to improve upon the properties of the matrix. An issue that arises is whether or not the full potential of the fiber reinforcement is being used? Or if, through some aspect of the composite manufacturing, the fiber's beneficial properties are reduced.

A common cause for fracture in Nextel™ 610 fibers has been observed to be weld lines [10]. These weld lines are believed to result from fiber processing, where two fibers are in contact with one another, likely during the sintering stages of the manufacturing process. Granted, this is a flaw that has been observed during fiber manufacturing, but fibers within a bundle or tow are very likely to be in contact with one another during composite processing. Particularly in the case of MetPreg™ tape, where continuous fibers are pulled through a molten bath of aluminum metal, the matrix forms by infiltration and wetting which does not guarantee that every single fiber is surrounded with the metal. It is difficult to determine how much of an effect fiber contact has, but is

an observation that should be considered when comparing the in-situ strength measurements of Nextel^{TM} 610 fibers to the individual fiber strengths.

Another aspect in regards to Nextel^{TM} 610 specifically is the fact that these fibers are designed and manufacturing parameters carefully controlled to produce a fine grained microstructure, which in part is the reason for this series of fiber displaying such high strength characteristics. So, grain growth within the fibers would be an issue of interest. Through manufacturing processes, the composite formation as well as products made from MetPreg^{TM} itself, the fibers will be exposed to elevated temperatures. In some cases it is very localized and limited, such as the tape placement method. Granted, alumina is used because of its high temperature capabilities, but in general there may still be a possibility for grain growth, which in turn could lead to a reduction in the properties of the reinforcement.

Chapter 2: Research Objectives

Nextel™ 610 fibers are added to the aluminum matrix of MetPreg™ composites for the main purpose of strengthening. However, there has not been extensive study into whether or not composite processing affects the strength of the fiber reinforcement. So, in an effort to characterize fiber strengths within the aluminum matrix (in-situ), a study of individual fiber strengths prior to composite manufacture will be established. The strength of individual Nextel™ fibers can be measured through tensile testing until fiber failure. By examining these individual fibers after failure, it is expected observable flaw sizes can be obtained from the fracture surfaces. Quantification of a characteristic fracture pattern referred to as fracture mirrors will be the basis of fracture examinations.

Establishing that a fiber has a visible flaw, the fracture mirror is measured to determine a critical flaw size. This flaw size information can then be applied to basic fracture mechanics through the use of the fracture toughness equation in an effort to establish a correlation factor between measured flaw sizes from fracture mirror observations to measured individual fiber strengths. The correlation based upon experimental data can then compared to a theoretical correlation, based upon material constants involved in the fracture toughness equation. In turn, the established relationship between flaw sizes on individual fibers to individual fiber strengths will be extended to determine the individual fiber strengths of fibers within the MetPreg™ composites.

Taking the data obtained from MetPreg™ examinations, an in-situ fiber strength distribution can be developed. This strength distribution can then be compared with the strength distribution of individual fibers, and observations can be made on the difference, or lack thereof, between the distributions. This evaluation can be viewed as a method for determining whether Nextel™ 610 fibers lose any of their strength characteristics due to the manufacturing process of MetPreg™ composites.

Chapter 3: Experimental Procedure

3.1 Fiber Sample Mount Design

A tow of Nextel™ 610 fibers was obtained from TRL for the purposes of this study. This fiber tow was the remainder of a lot that was used in the production of MetPreg™ tape. The Nextel™ 610 fibers could not be easily placed into the DMA grips, due to their small size and fragile nature. Through multiple trials, key aspects that came to light regarding the testing of individual fibers included fiber handling, successfully loading fibers for testing, and preserving fibers so that fracture surfaces of the tested fibers could be examined. As a result, a sample mount technique was adapted from a technique discussed through consultation from previous examination of Nextel fibers and modified to fit with this examination [11].

Providing support for handling of the Nextel™ 610 fibers, while still allowing for the ease of tensile testing with the DMA were of main importance. Index cards were cut to 2.5 cm in length and 1.5 cm in width, with a hole punched in the center. A one centimeter gauge length was marked in the center of the card piece, oriented parallel to the long side of the card. A fiber would then be glued into place at the gauge length marks using superglue. Once secured in the DMA grips, the card was then separated into two separate pieces through the use of a wood engraving tool. The paper was burned away, thus leaving only the fiber to be loaded during testing.

To preserve the fiber from shattering during fracture, the card mount was cut and altered such that a plastic tube was fitted into the hole in the center of the card mount. A fiber was then fed through the tube and glued into place at the one centimeter gauge length just like in previous tests. Once the glue had dried, a water-soluble lubricating gel was injected into the tube through the use of a syringe until the tube was full. Care was taken such that the needle of the syringe did not touch the fiber while injecting the gel. The new sample card mount was then set into the DMA testing grips and the card burned away such that only the fiber was loaded as before. Now with the gel around the fiber, successful tests were completed where a failure load could be measured and an associated fracture surface could be examined.

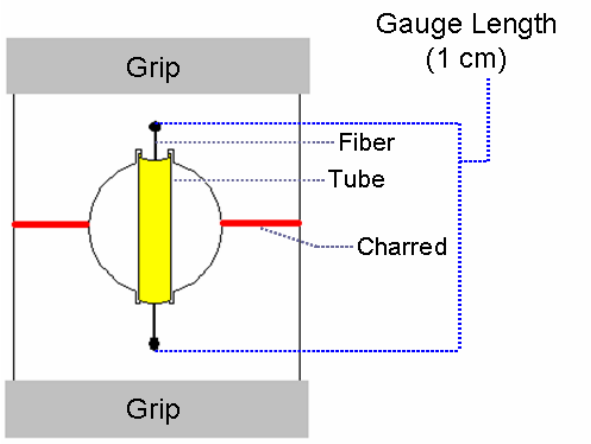

Figure 5 Schematic of sample card mount

3.2 Tensile Testing

The tensile testing of the Nextel™ 610 fibers was conducted with a controlled load on a Q800 series TA DMA with an 18N load cell using fiber/film tension test clamps. The fibers were tested using a controlled force mode with a constant stress ramp rate of 550 MPa/min to a maximum of 4000 MPa. After testing, the preserved fiber, still attached to one half of the card mount, was then cleaned to remove any excess gel that may have clung to the fiber. Since the lubricant gel was water soluble each fiber was gentle submerged in a water bath while holding the card mount with tweezers. The fibers were submerged until all gel that could be visibly seen was washed away. Lastly, the fibers were gently rinsed in an ethanol bath to remove any final globs of gel and dry the fibers.

3.3 Fracture Mirrors

Individual fibers that were successfully preserved from tensile testing were then taken to be prepped and examined in a scanning electron microscope (SEM). Of interest was determining if these fibers displayed an observable flaw on their fracture surface. Fracture mirrors are a type of flaw pattern that can be more readily discernable from fracture surface observations. Fracture mirrors are regions on the brittle fracture surface whose size is related to the critical flaw size that is the source of failure of the material. A fracture mirror is typically characterized by a smooth region on the fracture surface, which is associated with a stable or slow crack growth [12]. This area of crack

nucleation is then followed by a region of the fracture pattern referred to as the "mist." The mist region is a rough area along the border of the mirror region and separates the mirror from the "hackle." The "hackle" region resembles striations spreading from the mist outward across the fracture surface representing areas of fast or unstable crack growth during failure.

When examining the fracture surfaces of the individual fibers for fracture mirrors, the area of most interest is the mirror itself. The length *a* as denoted in the following figure is the flaw size that is measured. The mist and hackle regions are of interest mostly in determining the source of the flaw when a fracture mirror may not be easily apparent on the surface.

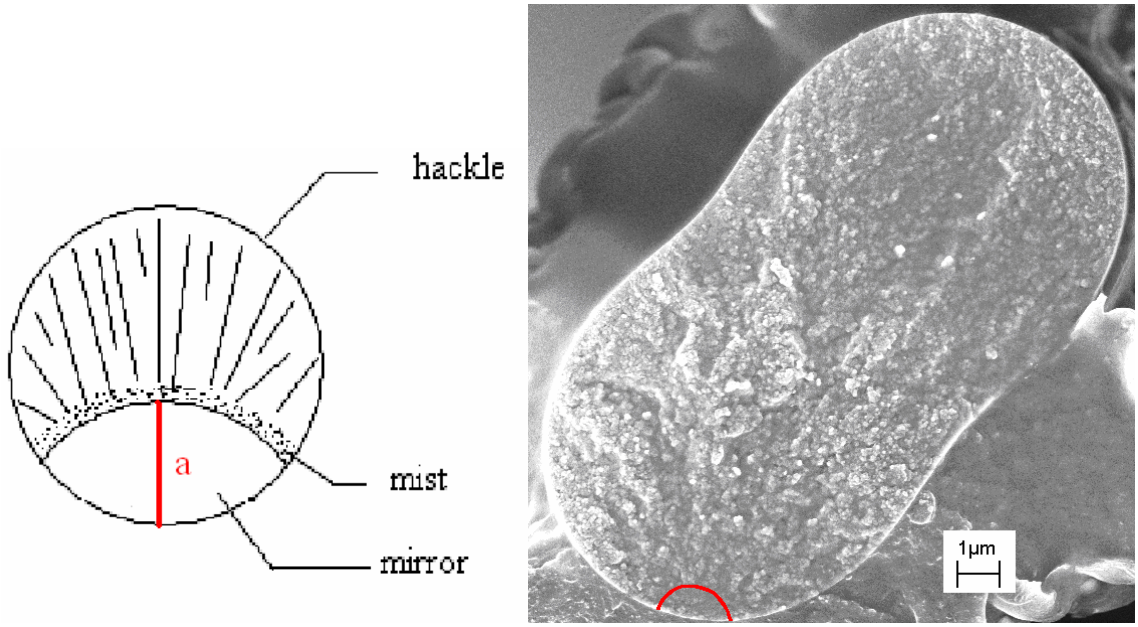

Figure 6 Sketch of a fracture mirror pattern on a circular cross section [12]. To the right is an SEM image of a tested Nextel™ 610 fiber exhibiting the mirror pattern.

3.4 SEM Examination

A means of obtaining images to properly characterize the surface of the fractured fibers was necessary. The diameter of Nextel™ 610 fibers is reported on the range of 10-12 μm [4]. It was apparent that available optical microscopy could not magnify the surface enough to properly observe and study the fracture surface. Also, the issue of handling the test fibers due to their small size arose. Proper placement and orientation of fiber samples for viewing in a microscope was necessary. As a result, SEM was used not

only for the ability to magnify the surface for a proper examination, but also for the capability of rotating the stage so that fiber samples could be viewed on end.

The tested single fibers were prepared by attaching an individual fiber to a SEM mount through the use of carbon tape. The fibers received a gold sputter coat of 7 nm to make them conductive. Images were first taken using the Inlens detector with a 5 kV voltage at 15000X and 30000X magnifications. At the 15000X magnifications the entire cross section of the fiber can be viewed. Upon examination, it became obvious that these fibers were not circular in cross-section, and thus the assumption used for determining the fracture strength needed to be adjusted. Thus it was necessary to take images at this magnification to be able use this image for cross sectional area measurement and to view the fracture surface to ascertain the presence of a fracture mirror. When an area on the fracture surface displayed a fracture mirror pattern, an image at 30000X was obtained for further investigation. The 30000X magnification yielded a closer examination of an area of interest on the fracture surface and was necessary in some instances where fracture mirrors were quite small. From these images, the size of a visible flaw was measured.

All images were examined and analyzed through the use of ImageJ software. This software was useful in its ease of use and ability to properly calibrate the pixel to length ratio for proper measurements. The 15000X magnification images were used to obtain the cross-sectional areas of the Nextel^{TM} 610 fibers, and these values were then used with the corresponding load at fiber failure to determine the strength of the each individual fiber. The 30000X magnification was used to determine the value of *a*, the flaw size for that particular fiber.

3.5 Analysis

For all the necessary calculations in this study, it was necessary to first obtain certain measurements from images of the fracture surface of the individual fibers. The main focus was in examining the fracture mirrors and measuring the flaw size, *a*, sometimes referred to as the flaw depth. Also, since the fibers did not display a circular cross section, it was necessary to measure the area of each of the tested fibers to properly determine the strength of the individual fibers with an associated failure load. The following SEM image shows an individual fiber that was examined. The area considered

as the fracture mirror is marked along with the length measured for the value of *a*, the flaw size.

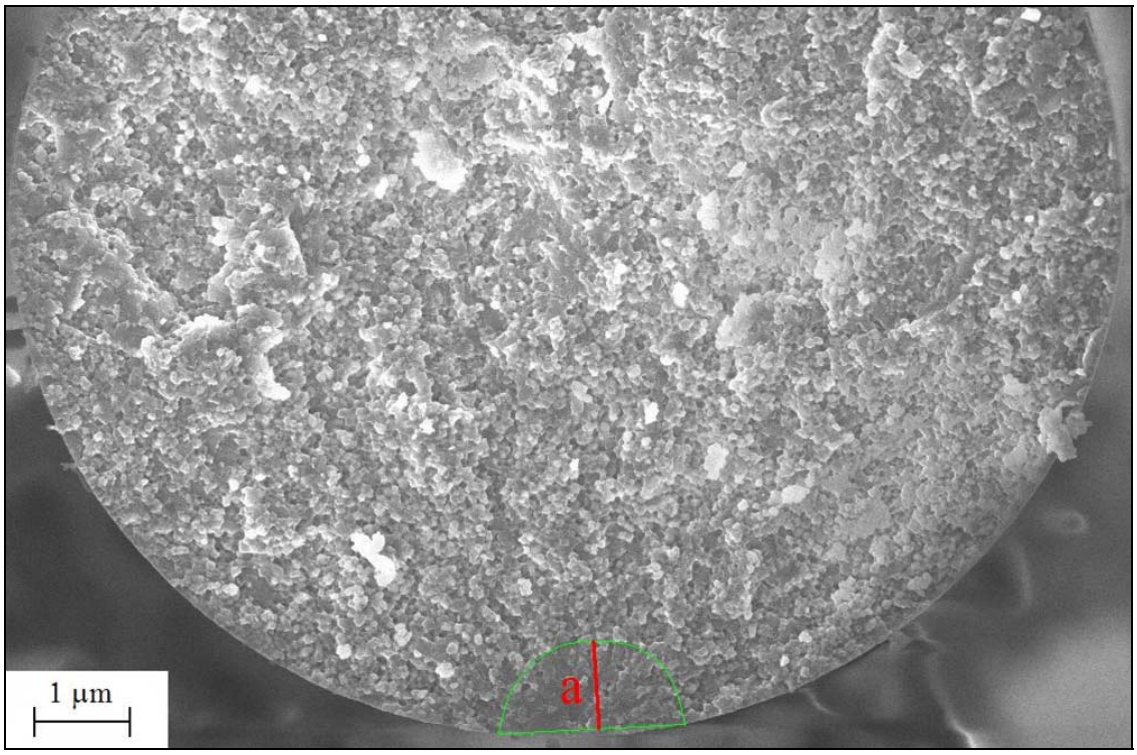

Figure 7 An example of an individual fiber with a fracture mirror. The length, a, indicated by the red line is the length measured for the determining the flaw size for this particular fiber. The flaw depth is determined from the surface edge of the fiber to the apex of the fracture mirror pattern.

After obtaining the cross-sectional area for an individual fiber, an individual fiber's strength could be calculated from its associated failure load obtained from DMA tensile testing. Analysis of the fracture strength data obtained through measurements was done by using Weibull statistics. To determine the Weibull modulus for the lot of Nextel^{TM} 610 fibers examined in this study, a pool of data points were obtained from testing of individual fibers at a constant gauge length of 1 cm. A distribution of single fiber fracture strengths is then determined from these calculations. It has commonly been seen that the quantification of a distribution of fiber fractures has been reported through the use of Weibull statistics [8].

The probability of survival for a given group of fibers is estimated by:

$$P_S = 1 - \frac{n}{N+1} \qquad \textbf{Eqn 1}$$

where N is the total number fibers whose fracture strengths were measured in the data pool and n is a position value assigned to the strength data point after the data was organized in ascending order. The P_S for each fiber with a measured fracture strength was then determined. The probability of survival data can then be fitted to a Weibull distribution:

$$P_S = \exp\left(-\left(\frac{\sigma_{\text{F, measured}}}{\sigma_o}\right)^m\right) \qquad \textbf{Eqn 2}$$

Where σ_F is a measured fracture strength of a fiber σ_o is a reference strength where P_S = 0.37 and m is referred to as the Weibull modulus. The Weibull modulus is indicative of the variability of the fracture data and can be determined analytically by manipulating the previous equation into a linear form for m as follows:

$$\ln\left[\ln\left(\frac{1}{P_S}\right)\right] = m \ln\left(\frac{\sigma_{\text{F, measured}}}{\sigma_o}\right) \qquad \textbf{Eqn 3}$$

Next, correlation between fiber strength and flaw size is determined. Developing a correlation between the single fiber strength data to the measured flaw sizes is based upon the fundamental fracture equation,

$$\sigma_{F,\,measured} = \frac{K_{IC}}{Y\sqrt{\pi a_{measured}}} \qquad \textbf{Eqn 4}$$

The fracture toughness, K_{IC}, is a material constant and the Y term is a geometric constant. The equation can then be rearranged and the constants, K_{IC}, Y, and π, are all combined together into an empirical correlation constant denoted by the C term in the following equation:

$$\sigma_{F,\,measured} = C\left(a_{measured}\right)^{-1/2} \qquad \textbf{Eqn 5}$$

The fracture strengths and the flaws on the fracture surfaces can both be measured in the case of individual fibers. This data can then be plotted, and the slope of data points determines the value of the empirical correlation constant, C. In turn, this C value is applied along with flaw sizes measured from fibers within a MetPreg™ sample to determine in-situ fiber strengths within the aluminum matrix.

3.6 MetPreg Examination

Study of MetPreg^{TM} samples followed a very similar overall procedure to that of the single fibers. MetPreg^{TM} strips were tensile tested until failure, and then the fracture surface was examined through an SEM. For tensile testing, the MetPreg^{TM} strips had to be altered to be properly gripped in the testing machine. Shims of aluminum metal were cut and attached to the MetPreg^{TM} samples through the use of an epoxy. Each of the aluminum shims were cut to 51 mm in length and the length between each shim being 127 mm, making the total length of a single sample 229 mm. A schematic of the samples including the aluminum shims that were tested can be seen in the below figure.

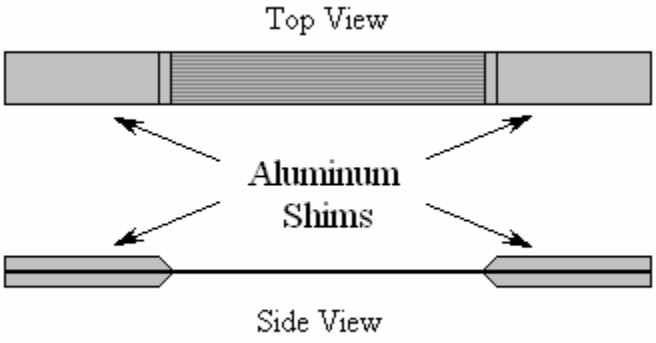

Figure 8 Sketch of MetPreg samples that were prepped for tensile testing.

The MetPreg^{TM} samples were tested on an Instron 4468 testing machine with a load cell of 50 kN at a strain rate of 2.6×10^{-4} s^{-1} until failure. Upon failure the fractured end of the MetPreg^{TM} tape was recovered and prepped for examination in the SEM. The fibers were attached to SEM sample mounts using carbon tape and then sputtered with a 7 nm coating of gold.

Once in the SEM, the samples underwent the same examination as the individual fibers. The fracture surface was studied to find fibers that displayed a characteristic fracture mirror pattern. Images were taken of fibers observed to exhibit fracture mirrors on their surface at 15000X and 30000X magnifications as in single fiber examinations. These images were in turn analyzed to determine the size of flaws and the cross sectional area of the observed fiber. The empirical correlation constant developed from single fiber examinations is then applied to the gathered flaw size measurements to calculate in-situ strengths of the fibers.

Chapter 4: Results

The majority of the fibers in the tow of Nextel™ 610 fibers examined in this study did not display circular cross-sections. Instead, due to a situation that arises in the drying step of sol/gel produced fibers, the fibers display a unique ellipsoid shape. This inconsistency in shape was observed in the MetPreg™ samples where the majority of fibers exhibited the ellipsoidal shape but on occasion displayed a few circular fibers. Figure 9 displays an image of a MetPreg™ sample with varying shaped fibers. Figure 10 which follows is a comparison between the cross sectional shapes of two individual Nextel™ 610 fibers that were studied.

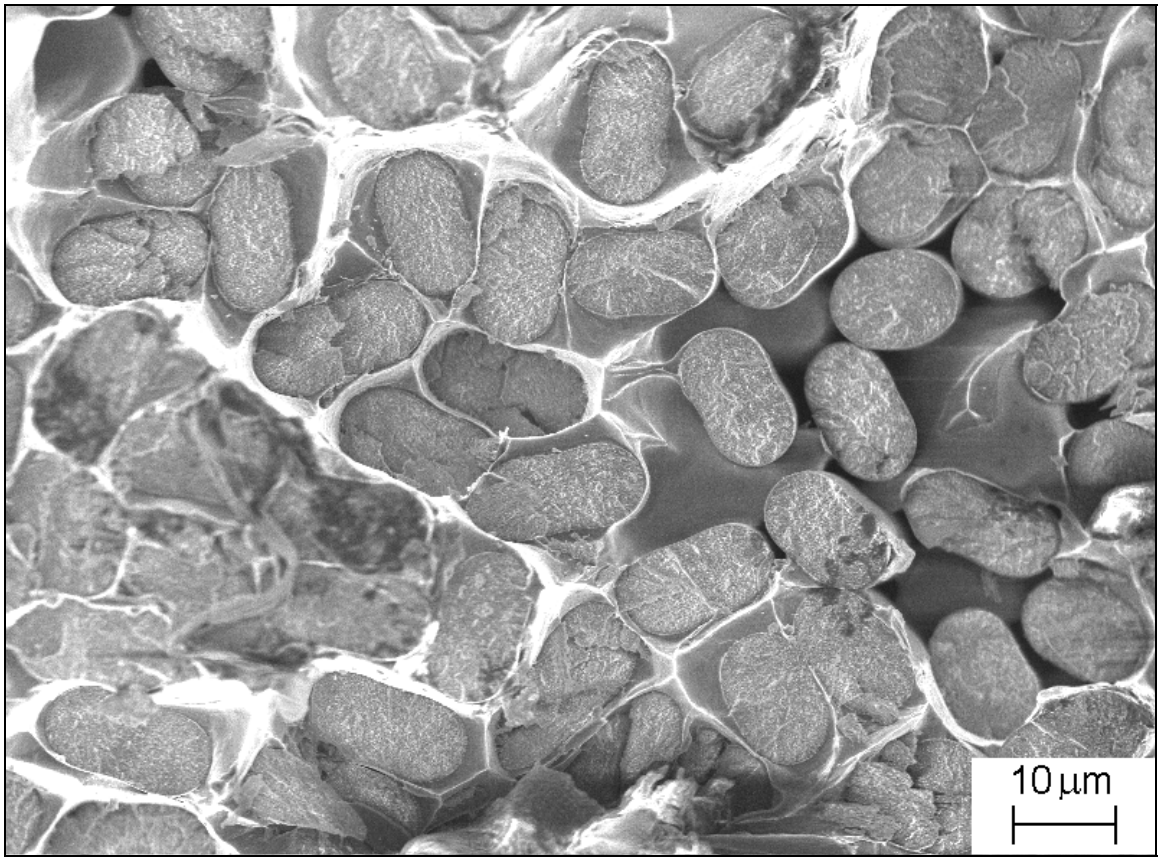

Figure 9 Image of a section of a MetPreg™ sample. The majority of the fiber reinforcement exhibits the ellipsoid shape, but it is noted that there are some fibers that are circular in cross section. This SEM image was taken using an Inlens detector with 5.0 kW at 2500X magnification.

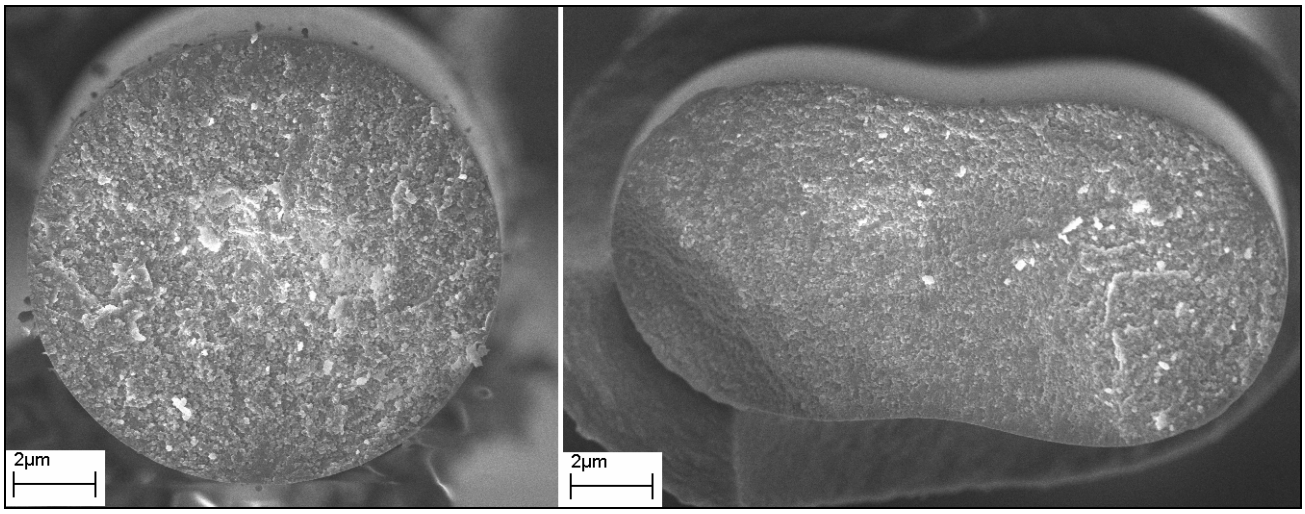

Figure 10 Shape comparison of Nextel™ 610 fibers. The image on the left is an example of a fiber displaying a circular cross-section. On the right is an image of the unique ellipsoid shape that was observed in the tow of fibers studied. Less than 1% of the fibers examined in this study displayed a circular cross section. Both images were taken using an Inlens detector on SEM at 15000X magnification at 5.0 kV.

Figure 11 shows the gathered data displayed in a Weibull plot. The value for m was found to be 2.4 for this data pool. After all the flaw size measurements and individual fiber fracture data are tabulated, the information is used to develop a value for the empirical correlation constant for Nextel™ 610 fibers. The gathered data is plotted using the trend displayed by Equation 5 and can be seen in Figure 12.

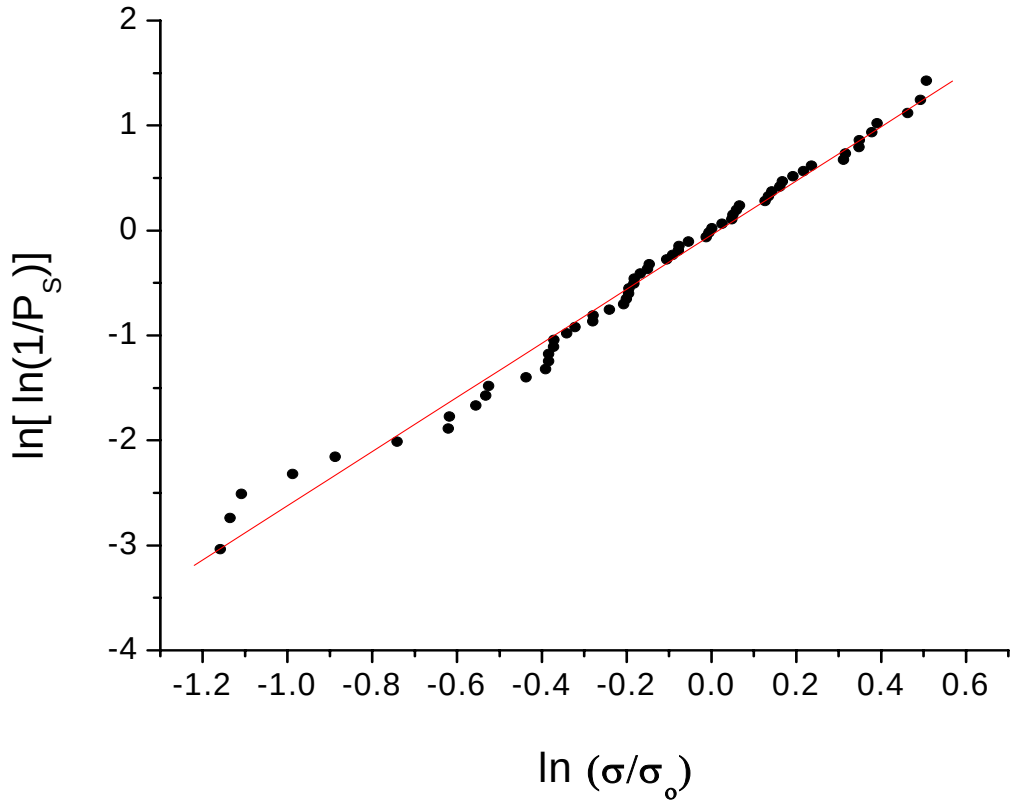

Figure 11 Weibull plot of probability of survival as a function of failure stress for individual fibers from the same lot.

An examination of a specific fiber's strength and its associated flaw size was important in order to determine the relationship between these two characteristics. From the relationship developed from single fiber data, it is hoped to apply this correlation to in-situ fibers within MetPreg^{TM} composites. The strength of individual fibers was plotted versus flaw sizes. In the plot of this data, it can be seen that there is a wide amount of variation in the points. A statistical value for determining the strength of a relationship between two variables is the correlation coefficient, commonly referred to as the r-value. The closer the value is to 1 or -1, depending upon the slope of the data, the stronger the relationship between the two variables being examined. The r-value determined for this plot of data between flaw size and fracture strength of individual fibers was found to be approximately 0.66, which displays a relationship that is not necessarily very strong.

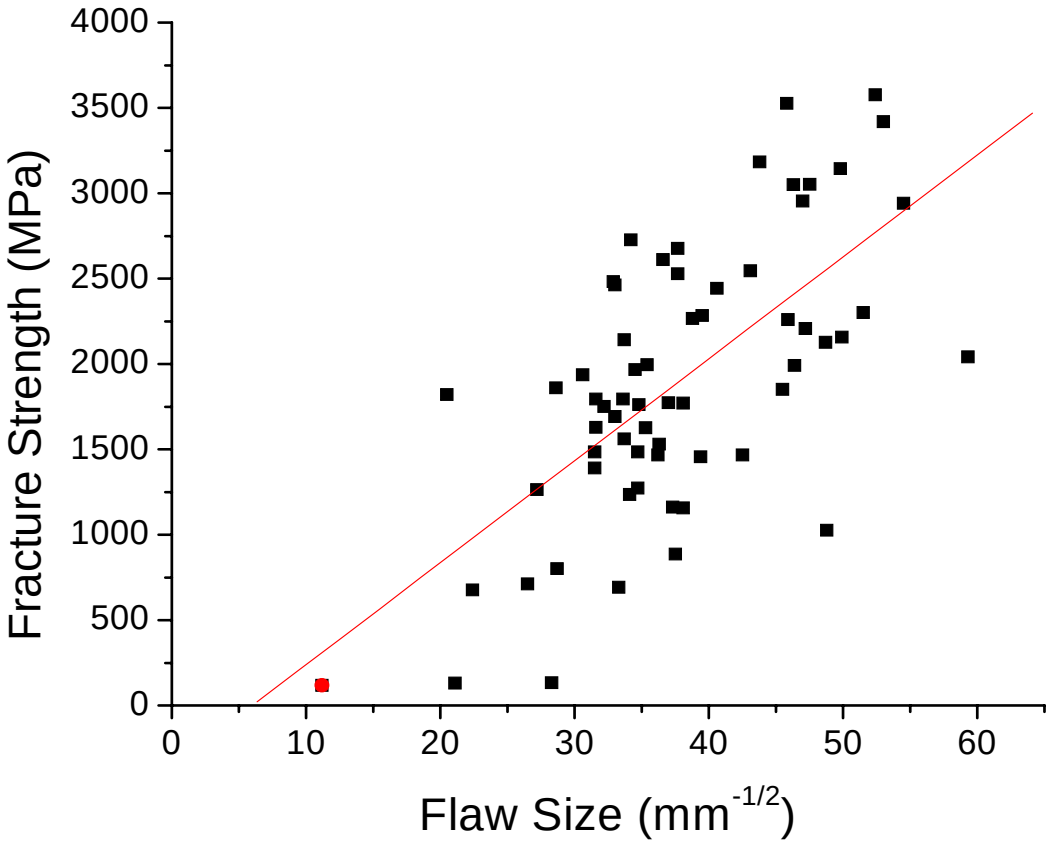

Figure 12 Plot of individual fiber fracture strength data vs the inverse square root of measured flaw sizes. The slope of the data is the empirical correlation constant, C. The red data point represents a fiber that failed at a relatively low fiber load during early testing, but the fiber was not preserved. So using an average fiber area and assumed the flaw size was the width of the fiber so that it may be included. The inclusion of this point was as a guide regarding the trend of the data.

Due to issues with image analysis and the polycrystalline nature of the material, it was difficult at times to clearly define the fracture mirror distance. Those flaws that displayed very distinct and clear fracture mirror patterns were denoted with a 'high confidence' level, representing a clear fracture mirror displayed on the fracture surface. Those values were plotted in the same manner and a new relationship was determined. The r-value for these points was found to be equal to 0.87, which displays a much stronger relationship between flaw size and fracture strength than with the compiled single fiber data.

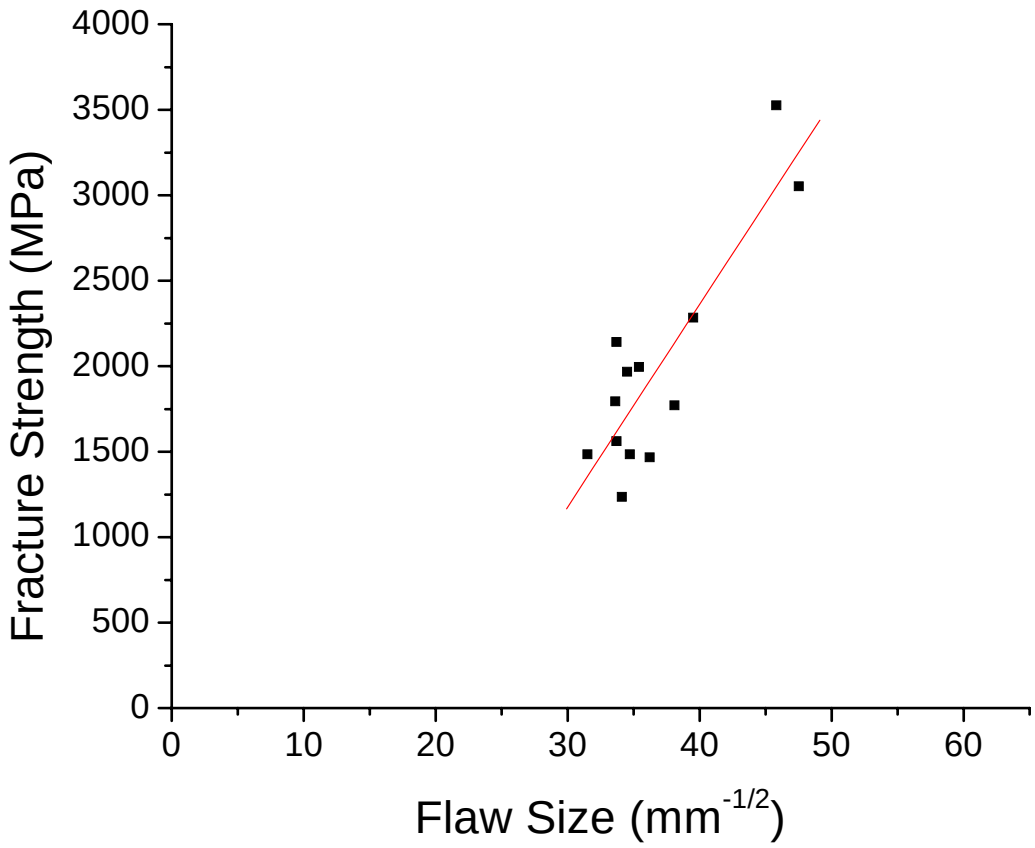

Figure 13 This plot of data is made of measurements that were deemed to have a high confidence in its measurement accuracy.

These two data plots have a distinct difference. As a result the empirical correlation constant will be different depending on which data set is used for its development. The slopes differ greatly, with the compiled data plot having a slope of approximately 59.7 and a slope of 118.4 for the high confidence data plot. Granted, the plot of the compiled data is more representative of the information gathered in this study, the high confidence plot displays points with a greater confidence in ascertaining their respective flaw sizes. To characterize and compare these experimental values, a theoretical empirical correlation, *C*, for this material can be calculated. Using the equation previously established, the value of *C* is as follows:

$$C = \frac{K_{IC}}{Y\sqrt{\pi}} \qquad \textbf{Eqn 6}$$

The K_{IC} value used for this calculation is 4.0 MPa*$m^{1/2}$ for near pure alumina [13] and the value for the geometric constant Y of the fracture mirrors was assumed to be 0.728

for the semi-elliptical surface crack situation [14]. This value is based upon a flaw geometry resembling a section of a circular arc whose center is located on the surface of round shaft. The limit for this assumption is based upon the ratio of the flaw depth, a, to the diameter of the shaft, d. For this study, the depth of the flaw size is easily measured, but due to the irregular shape of the fibers, the value for the diameter for these fibers was assumed to be the width of the ellipsoid section in which the flaw was situated. This can better be observed in the Figure 14.

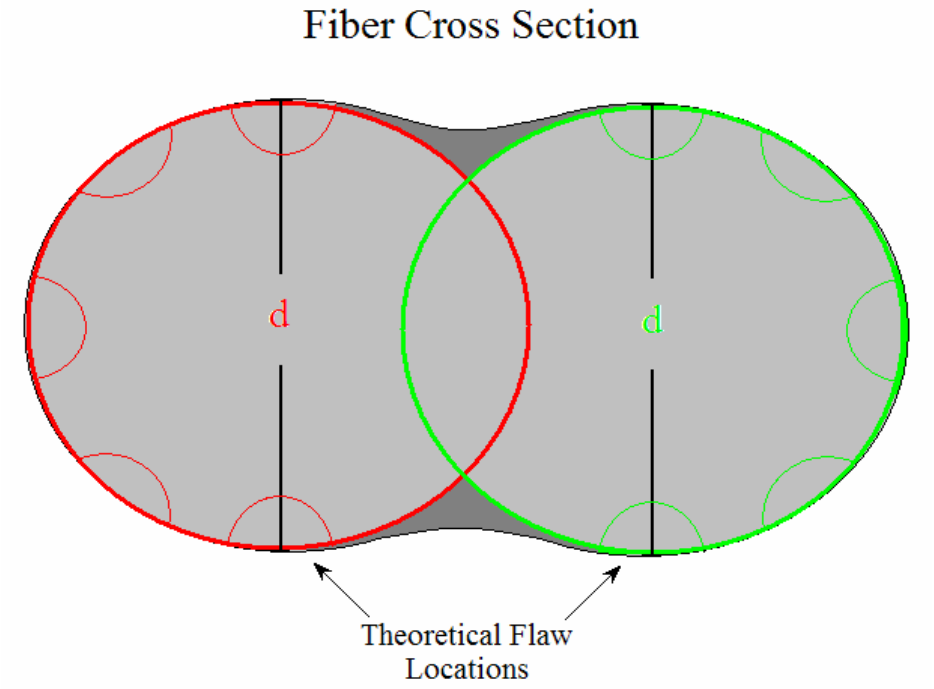

Figure 14 Schematic displaying how the value for d was assumed for the determination of the limit for the geometric constant of a given semi-circular surface flaw on a fiber. The majority of fracture mirrors were observed on the outer curves of the ellipsoid shape, so the corresponding d was measured for the flaw location. The only inconsistency pertained to flaws that were located more in the dark areas.

After assuming an appropriate value for d, the a/d for each individual fiber tested was determined. The value for the geometric constant is still within 10% of the assumed value as long as the ratio of $a/d < 0.30$. Since all tested fibers had an associated value of $a/d < 0.30$, it is assumed the value for $Y = 0.728$ is appropriate for these calculations. Substituting the values in for the material constant K_{IC} and the geometric constant Y, the theoretical empirical correlation for near pure alumina is found to be:

$$C = \frac{4.0}{0.728 \times \sqrt{\pi}} = 3.1 \text{ MPa } \sqrt{\text{m}}$$

$$= 98.0 \text{ MPa } \sqrt{\text{mm}} \qquad \textbf{Eqn 7}$$

Comparing this theoretical value of 98.0 $\text{MPa}\sqrt{\text{mm}}$ to the two values developed from experimental data, it can be seen that the compiled data value of 59.7 $\text{MPa}\sqrt{\text{mm}}$ is much lower while the high confidence data value of 118.4 $\text{MPa}\sqrt{\text{mm}}$ is closer to the theoretical even though it is higher.

Using the empirical correlation constant developed by the high confidence data, it can then be applied to flaw sizes measured from fibers within the composite matrix. The strength values that were calculated for fibers within the MetPregTM composites samples were observed having a greater average strength than that of the strength values obtained from individual fiber testing. Figures 15 through 17 are strength distributions of the entire single fiber data set, high confidence single fiber data, and the in-situ measured fiber strength as based upon a C = 118.4 $\text{MPa}\sqrt{\text{mm}}$.

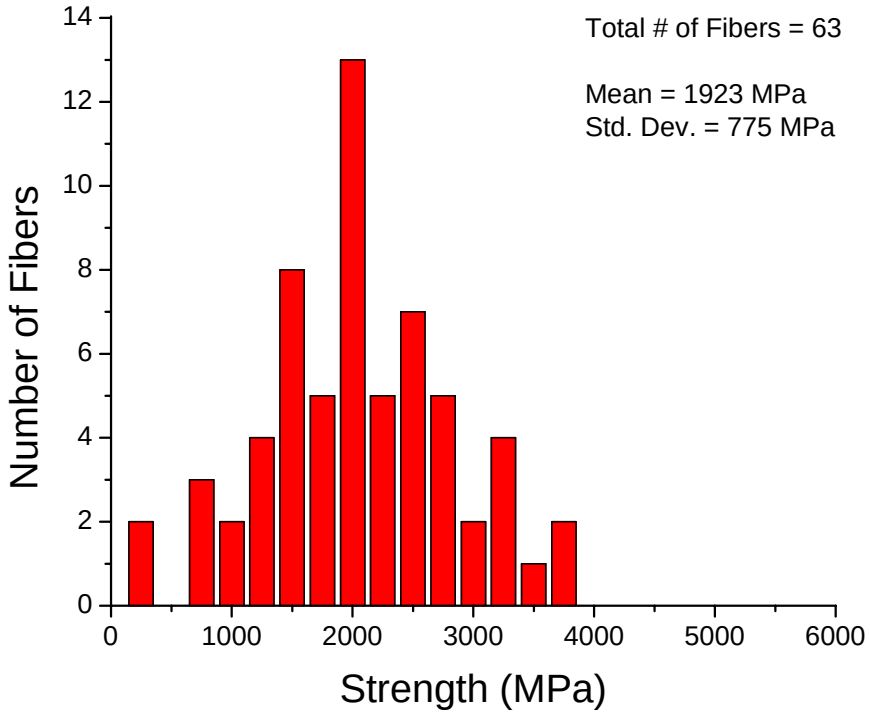

Figure 15 Strength distribution of all data points involved with single fiber testing.

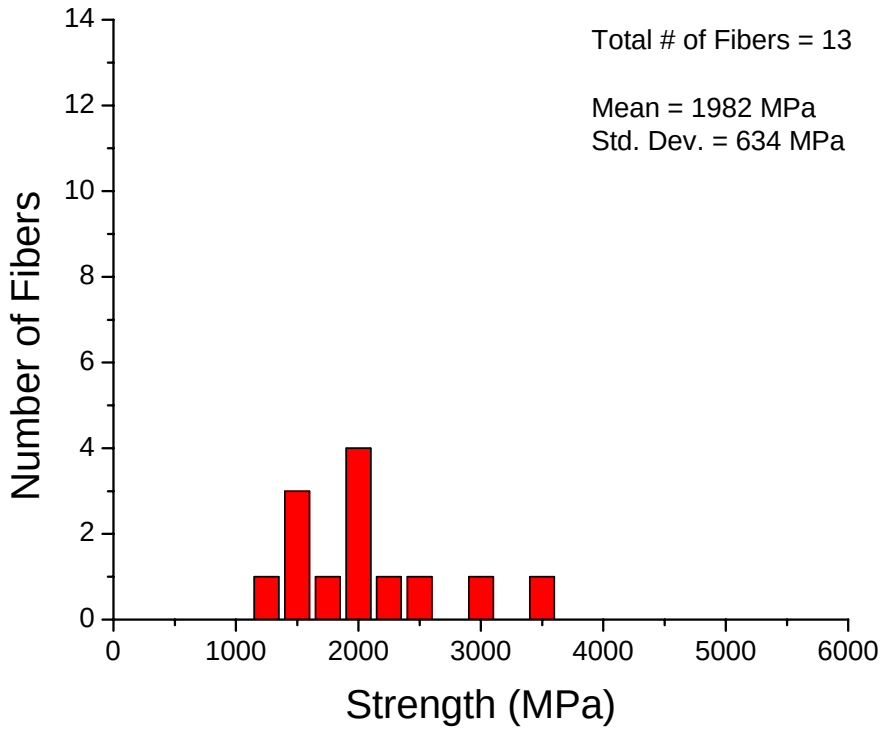

Figure 16 Strength distribution of the single fiber data with a high confidence association.

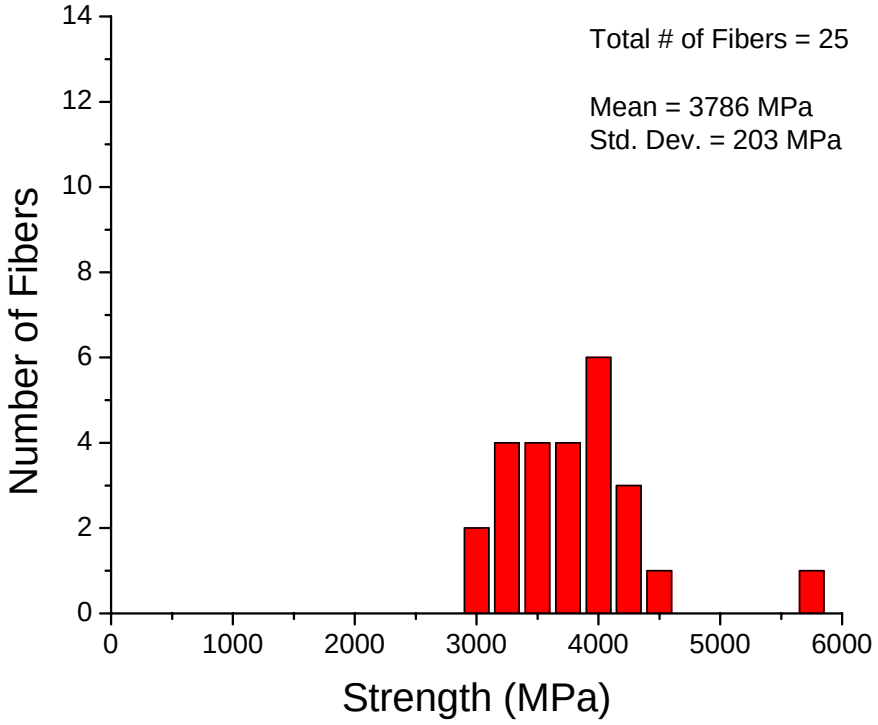

Figure 17 This strength distribution is a result of the fracture strength values generated with the correlation constant, *C* = 118, and measured flaw sizes from fibers within MetPreg™ composite.

Chapter 5: Discussion

Overall, the data that has been gathered has displayed a certain degree of scatter and variation when plotted. To better understand and explain this scatter, possible sources for variation in the data should be categorized. By categorizing the type of variation that can affect the data, it can then be determined if the scatter that resulted in this series of tests could be fine tuned with continued experiments or if the scatter in the data presented thus far is a result of inherent qualities pertaining to this material and experimental method. The categories for sources of variation can be broken down into the areas of testing technique, measurements, and inherent fiber qualities.

5.1 Testing Technique

The testing techniques used in this study contain aspects of the methodology to which care must be exercised. The importance of handling involved with the testing of individual Nextel 610^{TM} fibers cannot be stressed enough. These small fibers are delicate and were found to be quite fragile when preparing them to be tensile tested in the DMA. Attention should be paid to not introduce flaws to the fibers themselves so that they fail by a critical flaw size that is of interest and not by a flaw that may have been introduced to the material by handling.

In regards to tensile testing, the method adapted to this study has some similarities to methods observed in other research involving Nextel 610^{TM} fibers, which were in turn based upon ASTM standards for tensile testing of single filaments [10, 15]. The testing method contains aspects that should be taken into consideration as sources of variation. For instance, how the paper was cut to shape for sample mounts. The direction in which the paper cut is important because depending upon which side the hole is punched out in the center, the exit side of the punch can leave a raised edge to the paper. Then if a fiber is glued to a paper mount on the side with the raised edge from cutting, it can cause a contact point for stress and the fiber will likely fail at that point. In regards to the superglue, there was some evidence slippage occurred during a few tensile tests, when fibers slipped out of glue for a moment. Overall these instances did not appear to alter the failure load since the elastic behavior of the stress-strain curve stayed constant before and after the slip occurred, but this should still be mentioned as a source for variation.

Another aspect is ensuring the fiber is glued in place perfectly straight after being fed through the tube. In this study, marks were drawn in place on the card mounts as guides, but it is still important to note that a straight fiber is necessary for proper loading to occur in tensile testing. Also, the type of glue used to hold the fiber to the paper is important. It was observed that superglue with a gel consistency was more effective over the common liquid superglue, allowing for a better hold of the fiber on the paper.

All these aspects involved with the sample preparation and testing technique could be monitored, and therefore could possibly reduce the variation in further tests. Now, with this understanding, a comparison to other methods observed for the testing of Nextel 610^{TM} fibers is interesting to note. The Weibull modulus, m = 2.4, calculated from the current data is considered low in comparison to modulus values, m = 10.1 and 10.5, that have been reported for Nextel^{TM} 610 fibers [10, 15]. However, the fact that the testing methods were different between those studies and the one presented here should be considered when comparing the Weibull modulus values. Differences between the testing apparatus used, method for gripping the fiber for testing, and gauge length should all be considered. Though different in comparison to values found in other research, the Weibull modulus obtained here is representative of the data gathered in this study by this particular testing technique.

5.2 Measurements

The different measurements that were necessary for the development of the data presented in this study can all be sources for variation. It is of interest to examine methodology involved with each type of measurement and the data that resulted from them to ascertain the amount of variability that could be introduced, and then address each situation accordingly. The fracture load, cross-sectional area, and flaw size measurements are all aspects to be examined for possible sources to introduce variation into the data, as well as information that is based upon these measurements.

The failure loads obtained for each single fiber were subsequently used to calculate the strength of each fiber. It has already been examined with regard to testing technique how a failure load measured may not accurately represent the fibers due to induced flaws from handling and sample preparation. Therefore, aspects regarding the

accuracy of measurements from tensile testing should be considered. The testing clamps used were tension grips for fibers/films. This set of clamps was calibrated before each session of tensile testing, not before every single tensile test. Though unlikely, perhaps error could be introduced to measured values over time with multiple measurements as more and more tensile tests were conducted in a single session. At the very least, this aspect can be categorized as a source of variation for measurements.

The images obtained of the tested single fibers were an important step for determining the measurements associated with the fibers in this study. Yet the SEM images themselves can be regarded as a source of the variation. These fibers did not exhibit a circular cross-section as was expected, but instead displayed an ellipsoidal shape. Thus to more accurately measure the strength for a single fiber, the cross sectional area for each fiber was measured instead of assuming a circular cross section. This area in conjunction with the associated measured failure load determines the strength of an individual fiber. The resolution can affect the view of a fiber cross section and how detailed the fracture surface may appear, thus altering the interpretation of a fracture mirror. The orientation of the fibers themselves within the SEM was an issue when obtaining images. In some cases, the way a fiber was positioned on the carbon tape did not allow for a perfectly 'on end' view of the cross section in the SEM due to the tilt limit of the sample stage. This meant that the fracture surface was viewed at an angle, and when the area was measured, the value would vary depending upon how skewed the image would be of the fiber cross section.

So, what effect does this measured area that may be based upon a skewed image have in the determination of the Weibull modulus? As previously stated, the Weibull modulus obtained in this study has been observed to be lower than that of values found in other studies. Of interest is understanding this difference between the modulus values and determining the reasons for it. If, for instance, fibers were measured to have cross sectional areas larger than they actually had, then the strength values for those fibers would have been calculated to be lower than their actual fracture strength. So the calculated strength values of the individual Nextel^{TM} 610 fibers obtained would be more varied than in actuality because strength values were calculated with area values that may

not have been exactly accurate. In regards to the Weibull modulus, *m*, this means that a lower value will be obtained due to the variation that has been introduced.

Knowing that the cross-sectional area of a fiber could be affected by variation, the flaw size measurements also based on SEM images should be considered. For instance, what constitutes the flaw size that should be measured for analysis? In terms of the fracture toughness equation used in this study, the flaw size, *a*, is measured from the surface of the member to the apex of the fracture mirror observed. Yet it has been observed in other research involving fracture mirrors, that the value for *a* was not measured from the surface of the fiber, but from an arbitrary point outside the fiber [12]. This point was based upon *a* being the radius of a circle, with the fracture mirror being some portion of this circle. Thus, the choice in what the value of *a* should be is a point of contention, and thus a possible source of variation.

The geometry of the flaws is another point of interest. A large portion of flaws observed in this study were surface flaws located on the convex portion of the ellipsoidal fiber. As such, the calculations involved with determining the choice of the geometric constant value used were based on the situation involving a circular member. Due to the small shape it was assumed that the limits of the depth to width ratio for circular members was appropriate for all fibers, but it may not have been necessarily correct for flaws located within the concave portion of the fiber shape. In this study, all flaws measured were within the limit condition for a semi-elliptical surface crack in a circular member, even those flaws whose location was on the concave portion of the fiber. However, recognizing the location of surface flaws from fiber to fiber as a source of variation for measurements is reasonable.

The quality of SEM images results in some subjectivity that relies on how clearly the fracture surface is presented and on the examiner measuring the fracture mirror. In some instances, fibers were regarded as not displaying a visible fracture mirror and theses are important for consideration. For these cases, it is assumed that a fiber failed at a high strength and had a resulting fracture mirror to small to observe and measure. On the other side of this, a fiber may have failed at such a low load that the majority of the fracture surface itself was the mirror [12]. The polycrystalline nature of Nextel^{TM} 610 fibers becomes a point consideration because of how the fracture surface can be

interpreted. This aspect, which is a result of the material itself, resulted in a challenge when determining the exact flaw length during image analysis because of the subjective nature of flaw pattern observations for fracture surfaces exhibiting non-distinct fracture mirrors. Variation based upon this subjectivity could be introduced into flaw measurements, which may be an explanation for the scatter that is visible in the plot of compiled single fiber data comparing the relationship of flaw size to individual fiber strength. As a result, the high confidence data plot was formed in an effort to display data points involving fracture mirrors that were clearly defined and did not have multiple interpretations. It was also done to observe if there was any reduction in the scatter and a consequent stronger relationship between flaw size and fiber strength.

Even with this difficulty associated with the surface texture, it still becomes important to note that not all images necessarily displayed a characteristic fracture mirror pattern. Approximately 50% of the fibers that were tested and then underwent subsequent SEM examination displayed measurable fracture mirrors. There are a few explanations for this phenomenon. One obvious issue was that on some occasions, there was residual gel from the fiber preservation step still on the end of the fiber, obscuring the view of the surface. This was remedied with a more thorough cleaning process after tensile testing. Barring these exceptions, the percentage of fibers with measurable fracture mirrors increases to 60% of those tested. The remaining group either simply did not display a visible fracture mirror on the surface, the flaw was too small to be discerned, or the fiber fractured from another flaw source other than a surface flaw.

Viewing that area and flaw size measurements hold possible sources for variation, it is of interest to further explore the results that are developed based upon this information. Determination of the empirical correlation constant, *C*, is a key objective for this study. This value is what links the strengths of the individual Nextel^{TM} 610 fibers to the measured strength of fibers within the MetPreg^{TM} composite. The confidence in this relationship is the basis for determining an in-situ fiber strength distribution and the subsequent comparison to the individual fiber strength distribution.

The single fiber test data is a step in developing the empirical correlation constant, *C*, which ultimately leads to determining an in-situ strength measurement of fibers within the MetPreg^{TM} composite. So, reasoning behind the choice in the value for the empirical

constant and the differences between the theoretical and the value used should be justified. Foremost, the r-value determined for the compiled single fiber data was found to be 0.62 whereas the r-value for the data points deemed to have a high confidence was 0.87. The r-value is representative of the strength of the relationship between flaw size and fracture strength, so it seemed evident to go with the value that displayed the stronger relationship. The theoretical value for *C* was found to be $98\,\mathrm{MPa}\sqrt{\mathrm{mm}}$, which is based upon material constants. The value of $60\ \mathrm{MPa}\sqrt{\mathrm{mm}}$ gained from the entire data set differs greatly in comparison to the value of 118.4 for the high confidence data set. Though $60\ \mathrm{MPa}\sqrt{\mathrm{mm}}$ may be more representative of all the fibers in this particular study, it does not portray a strong relationship between the flaw size and fracture strength. As a result, the use of $118\ \mathrm{MPa}\sqrt{\mathrm{mm}}$ for the value of *C* is justifiable due to the stronger relationship of the variables in the high confidence data set and the fact that the value is closer to the theoretical. The only drawback to the use of this value for *C* is that, although confident of its greater accuracy over the $60\ \mathrm{MPa}\sqrt{\mathrm{mm}}$ obtained for the entire data set, the $118\ \mathrm{MPa}\sqrt{\mathrm{mm}}$ value does not necessarily represent a population of Nextel™ 610 fibers properly.

By using the $C = 118.4\,\mathrm{MPa}\sqrt{\mathrm{mm}}$, strength values were developed displaying higher values than those observed from individual fiber testing. After understanding the possible sources for variation based upon measurements, is the observation of higher strength for fibers located within the composite still justifiable? Although, with the justification of $118.4\ \mathrm{MPa}\sqrt{\mathrm{mm}}$ as the value for *C*, an argument regarding the small data population used for its determination can be made. The pool of data for in-situ strength of fibers within MetPreg™ is smaller than that of the individual fibers, a set of 25 versus 64 for the individual fibers. So, it can be argued that the in-situ fiber strength distribution may not necessarily be representative of fibers within MetPreg™ as a whole. Yet, all of these concerns can be addressed with further testing and enlarging the sample population for testing and calculations.

Therefore, it is of more interest to understand the trend observed in the data set obtained in this study. The main goal for designing a composite material is to attain better properties than using the constituent materials alone. The role of the continuous

reinforcement is for strengthening of the matrix and by the data gathered in this study it would appear that the reinforcement itself has had an increase in strength. This effect can be interpreted as the load transfer between the reinforcement and the matrix. With individual fibers, a fiber fails at its weakest point, but in the case with the MetPreg™ composite when a fiber fails at its weakest point, it does not necessarily mean failure for the material as a whole. When reinforcement fails, there will be an associated increase in the load experienced by the remaining fiber reinforcement and matrix, but assuming this increased load does not cause the fracture to further propagate through the material, the remaining matrix material and reinforcement share this increased load. As a result, the material will experience a higher load before complete failure.

Considering the small scale of these fibers, any minor variation in measurements could add up to large variation in the overall picture of the data. Area and flaw size measurements should be particularly monitored. This again is hinged upon image analysis, so acquiring quality images with respect to resolution and fracture surface detail is important. However, even with these opportunities for possible sources of variation, the results obtained in this study can, in some respect, still be justified.

5.3 Fiber Characteristics

Issues that are more inherent with the material may cause variation that cannot be altered, no matter how careful the testing technique or accurate the measurements. Certain fiber characteristics have been observed to be influential with testing and measurements. The small size of these fibers has been addressed as both a difficulty to testing and sensitivity towards measurements. Differences from one fiber to the next, not just with flaw distribution variations but flaw sizes, types of flaws, compositional differences, and even fiber damage during transport are all aspects that are outside of the controls of this study. Thus, the fibers themselves should be considered as a source of variation.

The fiber shape that has been observed in this study was a basis for sources of variation in measurements, but this aspect was not something that could be controlled in testing. The ellipsoidal shape of the fiber cross-section is a side effect of drying that results in fiber tows with a high denier, a denier being a term usually used for nylon or

silk fibers, where the standard is based upon a mass per length of 1 gram per 9000 meters. So, it is in tows where the mass per unit length is higher that this shape characteristic from drying is observed. This result of processing is not something that could be controlled within this study.

The majority of flaws observed in this study were surface flaws located on the convex portion of the ellipsoidal fiber. Yet, as mentioned with regard to measurements, flaws were also observed within the concave portion of the ellipsoidal fibers. Flaw location and the distribution of these flaws from fiber to fiber may or may not differ greatly. Thus the consistency of flaws from one fiber to the next in the same tow or bundle is an issue for consideration. Variability between the individual fibers could possibly be a source for inconsistency in the interpretation of results. For instance, variation in flaw distributions from one fiber to the next within a single tow was discussed in an article concerning the statistical strengths of Nextel^{TM} 610 and 720 fibers [10]. The scenario basically displays a narrow distribution of flaw sizes along the length of a single fiber, perhaps of a relatively small size. However, between different fibers the sizes could be very different. Figure 18 displays a schematic based upon the scenario described in Wilson's article regarding the different flaw distributions from fiber to fiber:

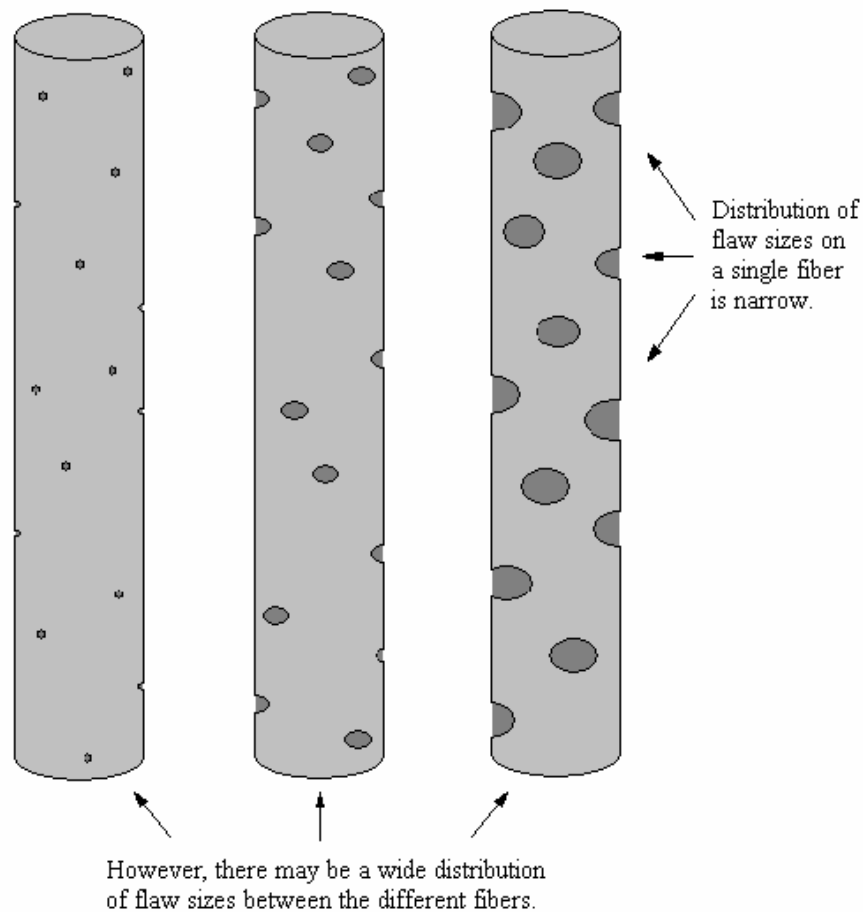

Figure 18 A schematic displaying the scenario of wide variation in flaw size distribution between fibers while maintaining a narrow distribution on the individual fiber itself. [10]

This situation leads to an aspect of the fiber testing that was not thoroughly examined. The gauge length used for testing the fibers was kept constant at 1 cm for all tests in this study. With the possibility of variation in flaw sizes from fiber to fiber, it can be inferred that the gauge length of the fibers can in turn affect the Weibull modulus. It has been proposed in other literature that by varying the size of the gauge length, the Weibull modulus would be higher since the measurement correlates more to the flaw distribution on the individual fiber as opposed to the flaw distribution between different fibers [10]. The Nextel^{TM} 610 fibers have a relatively large surface to volume ratio due to their small diameters. As a result of surface flaws being a source for higher stress concentrations than interior flaws, defects originating from a fiber's surface are more likely to be the controlling factor in a fiber's strength [15]. Normally, *m* is unaffected by volume effects such as gage length, however a case can be made here regarding not the

volume specifically, but the flaw spacing that could vary from fiber to fiber in the same tow. By separating out the fibers from a single tow and measuring them individually at a constant length, as in the case presented here, a wider distribution for the fiber strengths is obtained, and as a result a lower Weibull modulus.

With regards to image analysis, it has been pointed out that the polycrystalline nature of Nextel 610™ fibers can be seen and observations of the fracture surface can become a challenge because of this. The polycrystalline nature of the alumina was not conducive to determining the relative smooth area that is supposed to make up a fracture mirror. Due to its fine grain structure, the fracture surface has a rougher texture than compared with other fibers containing more silica. This roughness in texture made fracture mirror determinations more difficult. As a result, a portion of fibers examined did not display an easily discernable fracture mirror on the surface or there was evidence a fiber failed by a different flaw source than surface flaws. This last case was quite rare although did arise, and the following image is an example of an internal flaw from differing grain structure that was observed.

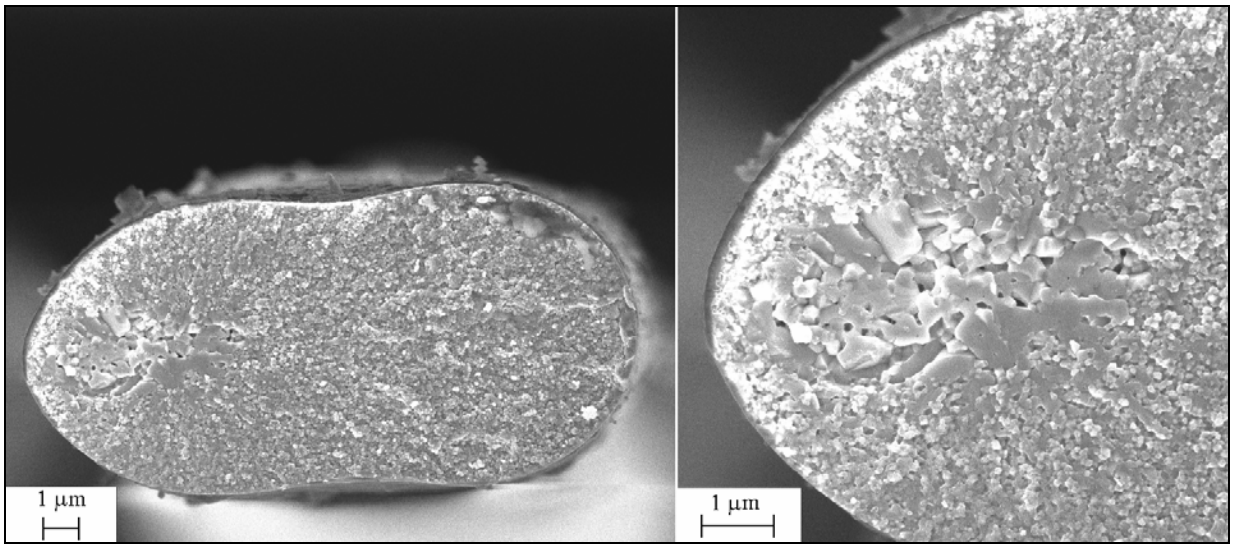

Figure 19 This fiber is an example of a fracture surface with no fracture mirror from a corresponding surface flaw. In this particular case there is an internal flaw observed by the inconsistency in the grain structure.

Chapter 6: Conclusions

The value of 2.5 for the Weibull modulus, though lower than expected, is justifiable. The testing method used for single fibers must be carefully monitored, to properly obtain valid failure values. Aspects, such as cutting the paper card mounts to reduce opportunity for edges to induce stress points on the attached fibers as well as attaching the fibers as straight as possible are important factors. Also, by eliminating the opportunity for variation in area measurements, the variation of values when determining the strength of fibers in single fiber testing can be decreased. By reducing this variation in strength values, it may in turn improve the relationship between the fracture strength and flaw size of Nextel^{TM} 610 fibers. With an improvement in the relationship, in effect a more accurate empirical correlation constant can be developed than the 60 $\text{MPa}\sqrt{\text{mm}}$ that was obtained for the compiled data.

The use of 118 $\text{MPa}\sqrt{\text{mm}}$ as the value for *C* is justifiable, due in part to the high confidence in the data used in calculating the value and its relative proximity to the theoretical value of 98 $\text{MPa}\sqrt{\text{mm}}$ compared to the 60 $\text{MPa}\sqrt{\text{mm}}$ for the compiled data. Also an important factor, the r-value of 0.87 displays a stronger relationship observed between flaw size and fracture strength in comparison to the 0.66 for the compiled data. As a result, there is a justified confidence associated with the strength distribution for in-situ fibers developed with the use of 118.4 $\text{MPa}\sqrt{\text{mm}}$ as the empirical correlation constant.

The greater strength values calculated for the in-situ measured strength distribution compared to the individually tested fiber distribution in effect displays the strengthening improvement by compositing. Likely due to load sharing between the matrix and continuous reinforcement, the reinforcements can experience a greater average load than the load experienced by a fiber tested individually. So, fibers within the matrix that survive the failure of their weaker members can experience a higher load, which explains how the distribution calculated for fibers within the matrix of MetPreg^{TM} composite is greater than that of the individual fibers that were tested.

Differentiating the sources for possible variation, further study of Nextel 610^{TM} fibers can be adapted accordingly. Variations that could result from testing technique

could and should be monitored closely for continued studies. The data presented here can be strengthened by further experimentation, either as proof that this method of testing has a certain degree of variation to it or that the aforementioned techniques are the sources for variation within the methodology. One point of interest from these experiments and data gathering, is that that future work should perhaps involve a more quantitative method for determining the area of a fracture mirror. A topographical analysis of the fracture surface perhaps through the use of a confocal microscope may be more beneficial in determining the fracture mirror, since a mirror is an area of relative smoothness on the surface of the fracture. By quantitatively differentiating between the area of a fracture mirror and the rest of the fracture surface, it removes the subjectivity that may have been introduced into the analysis of SEM images and subsequent flaw size measurements. An alternative method for fiber fracture examination may aid in determining exact fiber areas by increasing the ability to observe the fibers "on end." The small size associated with these fibers makes it difficult to simply examine the surface, therefore whatever the technique, the handling and preparation of the Nextel^{TM} 610 fibers for examination after testing may be a very involved process. Aspects inherent to the material itself cannot be controlled and thus variation effects from this source may still appear in the data. However, with proper methodology in place, it can be inferred that the resulting scatter from subsequent data would be something inherent in the material, and not from testing technique or measurements.

References

1. John W. Weeton, D.M.P., Karyn L. Thomas, *Engineer's Guide to Composite Materials*, ed. A.S.f. Metals. 1990, Metals Park, Ohio: Carnes Publication Services, Inc. 5.5-5.13.
2. Kampe, S.L., *Composite Materials - MSE 5104*. 2005, Virginia Tech.
3. Cooke, T.F., *Inorganic Fibers - A Literature Review*. Journal of American Ceramic Society, 1991. **74**(12): p. 2959-78.
4. 3M™, *Nextel™ Ceramic Textiles Technical Notebook*, in *3M™ Nextel™ Ceramic Fiber Typical Properties*. 2006.
5. Committee, A.I.H., *Engineered Materials Handbook*. Composites. Vol. 1. 1989, Metals Park, Ohio. 60-63, 117-118.
6. Reinhart, T.J., *Engineered Materials Handbook*, ed. C.A. Dostal. Vol. 1. 1989, Metals Park, Ohio: ASM INTERNATIONAL Handbook Committee. 60.
7. Wilson, D.M.V., L.R., *Nextel™ 650 Ceramic Oxide Fiber: New Alumina-Based Fiber for High Temperature Composite Reinforcement*, in *24th Annual Conference on Engineering Ceramics and Structures*. 2000: Cocoa Beach, FL.
8. D.M. Wilson, L.R.V., *High performance oxide fibers for metal and ceramic composites.* Composites: Part A, 2001(32): p. 1143-1153.
9. Virgil Irick, B.G., *MetPreg™ Metallic Prepregs for the Composite Industry.* SAMPE Journal, 2004.
10. Wilson, D.M., *Statistical Tensile Strength of Nextel™ 610 and Nextel™ 720 fibres.* Journal of Materials Science, 1997. **32**: p. 2535-2542.
11. Kampe, J. 2005: Blacksburg, VA. p. Consultation on single fiber testing technique.
12. R.H. Stawovy, S.L.K., and W.A. Curtain, *Mechanical Behavior of Glass and Blackglas Ceramic Matrix Composites.* Acta mater., 1997. **45**(12): p. 5317-5325.
13. *MatWeb: Material Property Database*. 2006, http://www.matweb.com/search/GetProperty.asp.
14. Dowling, N., *Mechanical Behavior of Materials*. Second ed. 1999, Blacksburg, VA: Prentice Hall. 286-311.
15. Chawla, N.K., M., *Monotonic and Cyclic Fatigue Behavior of High-Performance Ceramic Fibers.* Journal of American Ceramic Society, 2005. **88**(1): p. 101-108.

VITA: Joe Butler

Joe began attending Clemson University in the Fall of 1999. During his freshman year he was introduced to the materials field by Ceramic Engineering presentation through a general engineering course. During his time there, the Ceramic Engineering department went through changes to become a broader materials science program. For two summers he interned with Ceratizit Inc, a carbide alloy company where he worked as a lab assistant in quality control. He graduated from Clemson University December 2003 with a bachelor's in Ceramic and Materials Engineering. In an effort to further expand his knowledge in other aspects in the field of Materials Science, Joe decided to attend graduate school. The summer before coming to Virginia Tech he did some laboratory work and carbon fiber sample preparation for the Center for Advanced Engineering Fibers and Films at Clemson. He has attended Virginia Tech and been a student in the Materials Science and Engineering department since the Fall of 2004.

Outside of school, Joe is an avid gamer with a variety of interests from videogames to historical war games. Beyond that he’s a fan of fishing and enjoys hiking.